Engenharia Agrícola
ISSN: 1809-4430 (online)
www.engenhariaagricola.org.br | www.scielo.br/j/eagri

Scientific Paper
DOI: http://dx.doi.org/10.1590/1809-4430-Eng.Agric.v45e20240140/2025

RESEARCH AND OPTIMIZATION OF THE INCLINATION ANGLE DIFFERENCE OF THE DIGGING SHOVEL SURFACE OF POTATO HARVESTER IN HILLY AREAS

Chunyan Kong[1*], Qixin Wang[1*], Yi Liao[1], Jie Xia[1], Yangyang Jin[1]

[1*]Corresponding author. Xihua University, Chengdu, China.
E-mail: kongcy@mail.xhu.edu.cn | ORCID ID: https://orcid.org/0000-0002-2658-402X
E-mail: wqx1460078156@163.com | ORCID ID: https://orcid.org/0000-0002-6246-9125

KEYWORDS

potato harvester, digging shovel, shovel face inclination angle, angle difference, simulation optimization.

ABSTRACT

Due to the complex terrain and variable soil conditions in hilly areas, traditional potato harvesters often face challenges such as high excavation resistance, insufficient soil disturbance, and high crop loss rates. This paper, based on soil mechanics and the working principles of potato harvesters, uses EDEM (Discrete Element Method) discrete element software to simulate different combinations of blade angle differences, and systematically studies their on-excavation performance. The results show that the angle difference Δ_1 between blade angles α_1 and α_2, and the angle difference Δ_2 between α_2 and α_3, significantly affect excavation performance. Proper blade angle design can significantly reduce excavation resistance, enhance soil disturbance effects, and reduce power consumption. Specifically, blade pressure fluctuates with increasing angle difference; forward resistance significantly increases under conditions of large angle differences; and within a certain range of Δ_2, the blade operates with higher efficiency and lower power consumption. In summary, rational optimization of blade angle design can improve harvest efficiency and crop integrity.

INTRODUCTION

The operational efficiency and effectiveness of agricultural machinery are significantly influenced by the complex terrain and variable soil conditions in hilly areas (Wang et al., 2021; Wei et al., 2019; Wu, 2022). Potatoes, being an important cash crop, have a yield and quality directly related to the mechanization level of the harvesting process. However, traditional potato harvesters often encounter problems such as high digging resistance, insufficient soil disturbance, and high crop loss rates when operating in hilly areas (Bao et al., 2021; Cao et al., 2023; Xu et al., 2019). Therefore, optimizing the design of potato harvester digging shovels for the specific terrain conditions in hilly areas has significant practical importance.

As a key component in agricultural machinery, the design and optimization of digging shovels have been extensively studied both domestically and internationally. The traditional excavator shovel has the problems of poor terrain adaptability, low harvesting efficiency, and easy wear of excavation tools. Optimizing the structure and parameters of the shovel body can improve the excavation efficiency, reduce energy consumption, and improve the adaptability and stability of the operation. Recent international research has focused on innovative approaches to enhance the effectiveness and efficiency of digging shovels for potato harvesters. Thomas & Fischer (2020) explored the application of ultra-high molecular weight polyethylene (UHMWPE) coatings to reduce soil adhesion and wear on the blades. Müller & Schmidt (2019) conducted extensive field tests to evaluate the impact of shovel blade angle variability on the efficiency of soil cutting and tuber damage. Wilson et al. (2021) implemented advanced computational fluid dynamics (CFD) simulations to optimize the flow of soil and reduce the energy consumption of potato harvesters. Furthermore, Clarke (2022) investigated the use of hybrid metal-composite shovel blades, which significantly improved durability and flexibility under varying soil conditions. Domestic research focuses more on optimizing the design of digging shovels in conjunction with actual agricultural environments. Studies (Ge et al., 2023; Ye et al., 2023; Zhang et al., 2022) have shown that biomimetic design can significantly improve the

[1] Xihua University, Chengdu, China.

Area Editor: Fábio Lúcio Santos
Received in: 8-11-2024
Accepted in: 3-6-2025

performance of digging shovels. For instance, biomimetic digging shovels inspired by mole crickets' foreclaws and wild boars' rooting snouts have demonstrated excellent resistance reduction and soil-breaking capabilities during digging. Additionally, the interaction between soil particles and digging shovels has been simulated using the Discrete Element Method (DEM) to optimize the structural parameters of digging shovels, thereby enhancing digging efficiency and stability.

Although numerous studies have analyzed the digging shovels of potato harvesters, they have not considered the impact of the angle difference in the shovel face inclination on digging performance. This study focuses on determining the effect of the angle difference between the shovel face inclinations of potato harvesters on overall digging performance, aiming to enhance their operational efficiency in hilly areas and provide a basis for designers in selecting the shovel face angle. The shovel face inclination angle, a key parameter in the design of digging shovels, directly affects soil cutting, breaking, and lifting processes. Traditional designs of potato harvester shovels are often based on the conditions of plain areas; however, in hilly regions, due to variations in soil moisture and hardness, the design of shovel face angles often proves to be inappropriate, commonly resulting in uneven soil breaking, high forward resistance, and severe potato damage during operations, thereby affecting harvesting efficiency and potato damage rates (Park et al., 2019). A rational design of the shovel face inclination can significantly reduce digging resistance, improve soil disturbance effects, lower overall power consumption, and thus enhance harvesting efficiency and crop integrity (Wei et al., 2023). Therefore, optimizing the shovel face inclination of potato harvesters and determining the impact of the inclination angle difference on overall digging have significant implications for improving the adaptability and operational performance of potato harvesters in hilly areas.

In this study, we first established geometric and mechanical models of the digging shovel and soil based on soil mechanics and the working principles of potato harvesters. Subsequently, we utilized the EDEM discrete element software to simulate all combinations under different shovel face inclination angle differences, evaluating the design based on shovel face pressure, power, and forward resistance. We determined that the angle differences Δ_1 between shovel face inclination angles α1 and α_2, and Δ_2 between α_2 and α_3, significantly impact overall digging performance, thereby ensuring the effectiveness of the optimized design in practical applications. This research not only provides new ideas and methods for the design of potato harvesters in hilly areas but also offers a reference for optimizing the design of agricultural machinery under similar terrain conditions. By combining theoretical analysis with simulation, the study supports the enhancement of agricultural mechanization levels and potato harvesting rates in hilly areas, thus improving the mechanization level and operational efficiency of potato harvesters and reducing operational damage.

Shovel structure and main parameters

Shovel structure

Shovels can be classified according to their assembly style into fixed, driven, and combination types (Zbanov et al., 2020). A fixed shovel is rigidly connected directly or indirectly to the frame, moving synchronously with the digging device during operation. It offers good stability and wear resistance, effectively reducing the occurrence of missed potatoes during harvesting. In hilly areas, potato harvesters typically use fixed multi-blade shovels. Therefore, the shovel designed in this paper adopts a fixed assembly type and features a three-small-blade structure. The blade is designed with multiple segments, and the overall structure is shown in Figure 1(a). This structure performs excellently in terms of soil penetration, soil breaking, and loosening capabilities, and it also reduces the mound of soil accumulated during potato harvesting. The entire shovel uses a symmetrical design to ensure even distribution of stress and prevent local damage due to stress concentration. The structure of a single blade is shown in Figure 1(b).

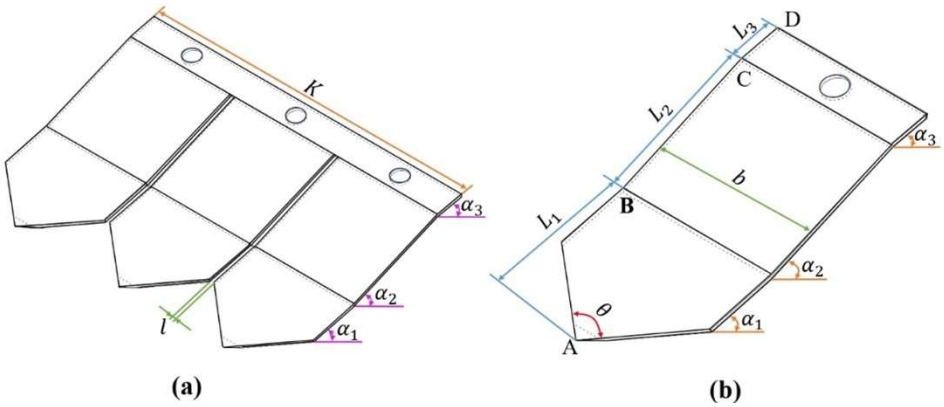

FIGURE 1. Structure diagram of the digging shovel. (a) Overall structure, (b) Single-blade structure.

Where:

α_1—Shovel face inclination angle in segment AB, °;

α_2— Shovel face inclination angle in segment BC, °;

α_3—Shovel face inclination angle in segment CD, °;

L_1—Shovel surface length in segment AB, mm;

L_2—Shovel surface length in segment BC, mm;

L_3—Shovel surface length in segment CD, mm;

b—Single shovel operation working width, mm;

θ—Shovel blade opening angle, °;

l—Shovel gap, mm;

K—Effective total width of the digging shovel, mm.

Main parameters of the digging shovel

The operating speed of a potato harvester refers to its forward movement speed. The digging shovel designed in this paper is intended for small plots in hilly areas and is primarily equipped with tractors of 50-70 horsepower. Therefore, the maximum operational speed of the tractor is set at v_0 = 1.2 m/s (Zhou et al., 2023).

Selecting the appropriate digging shovel entry parameters is crucial for effectively excavating the soil-potato mixture and transporting it to the soil-potato separation mechanism (Li et al., 2023). Considering the actual conditions of the soil in hilly regions, a mechanical model of the digging shovel has been established, as shown in Figure 2, and an analysis of the forces acting on the shovel after it enters the soil layer has been conducted.

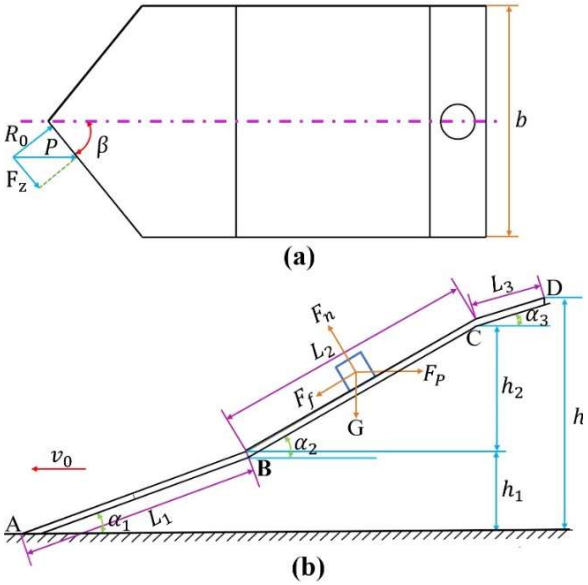

FIGURE 2. Force analysis of the digging shovel.

Where:

β —Blade opening angle, °;

P—Resistance force on the blade, N;

F_Z—Frictional force between the potato-soil mixture and the blade, N;

R_0—Force perpendicular to the blade, N;

G—Weight of the potato-soil mixture, N;

F_P—Force required to lift the excavated material along the movement of the digging shovel, N;

F_n—Support force of the digging shovel on the potato-soil mixture, N;

F_f—Frictional force of the digging shovel on the potato-soil mixture, N;

h_1—Depth of entry into the soil for segment AB, mm;

h_2—Depth of entry into the soil for segment BC, mm;

h—Total depth of entry into the soil for the digging shovel, mm.

Design of the digging shovel blade angle

The optimization of the shovel blade opening angle aims to reduce the sliding shear resistance between weeds and stems and the digging shovel. An appropriate blade opening angle not only reduces the forward resistance of the digging shovel but also facilitates the smooth transportation of the soil-potato mixture to the soil-potato separation mechanism (Dun et al., 2023). Additionally, the blade opening angle must ensure that stems and weeds can smoothly slide off the blade to prevent entanglement. In summary, the blade opening angle should meet the following formula (Wei, 2024):

$$F_Z < P\sin(90^\circ - \beta) \tag{1}$$

Based on [eq. (1)], it can be derived that $\beta < 90°$. Based on previous studies, (Tan et al., 2023; Yi et al., 2023) the friction coefficient between heavy clay and clay with steel ranges from 0.4 ~ 0.9. This paper selects the maximum friction coefficient of 0.9. Typically, β ranges between 44° and 52°. To meet the design requirements, this article selects β = 50°. According to Figure 2, $\theta = 2\beta$, therefore θ = 100°.

Design of the digging shovel width

The effective total width K of the digging shovel primarily depends on the subsurface distribution of potato tubers, row spacing, plant spacing, growth conditions, and deviations in the harvester's travel path (Wang et al., 2021). To ensure that all the mixture within the entire potato ridge is effectively excavated, the working width of the digging device should be slightly wider than the bottom width of the ridge. The working width K of the digging shovel can be determined using the following formula:

$$K = M + e + 3\sigma + 2c \tag{2}$$

Where:

M—Average row spacing, mm;

e —Average distribution width of potatoes, 200 mm~250 mm;

σ —Composite standard deviation, mm;

c—Machine travel deviation, 50~80 mm.

$$\sigma = \sqrt{\sigma_M^2 + \sigma_b^2} \tag{3}$$

Where:

σ_M —Standard deviation of row spacing, mm;

σ_b—Standard deviation of potato tuber distribution width, mm.

This study sets the following parameters: M = 300 mm, e = 200 mm, σ_M = 60 mm, σ_b = 60 mm, and c = 50 mm (Wang et al., 2023b). Considering the agronomic requirement for a maximum ridge bottom width of 800 mm, the digging shovel effective total width K equals834 mm. Given that the digging shovel designed in this paper features a fixed structure with three small shovels, [eq. (4)] gives the width of the shovel blade for each individual shovel as b = 270 mm.

$$b = \frac{K - 2l}{d} \tag{4}$$

Where:

d —Number of digging shovel blades in a single shovel body, $d = 3$;

l —Shovel gap, set as l = 12 mm.

Design of the length of the digging shovel

In hilly regions, potato tubers typically lie between 150 mm and 200 mm beneath the surface. To meet the growth requirements of potatoes and improve the cleaning rate, the total penetration depth of the digging shovel should ideally be between 150 mm and 220 mm. The digging depth has a significant impact on the traction resistance of the shovel at different blade angles. With fixed parameters for blade angle and soil properties, the deeper the digging depth, the greater the traction resistance of the shovel (Wang et al., 2023a; Xin & Liang, 2022); however, considering that a connection plate is installed below the shovel which can adjust the penetration depth, and the transport chain is situated below the ridge's top level, the actual digging depth of the shovel is about 170 mm. h_1 is the vertical distance from the connecting plate to the bottom of the bucket, which should be set according to the actual operation requirements to ensure that the connecting plate can effectively control the penetration depth and avoid equipment damage caused by digging too deep. h_2 indicates the initial position of the transport chain, which should be selected taking into account the position below the top level of the ridge in order to optimize the trajectory of the transport chain and ensure operational efficiency. h is the size of the gap between the connecting plate and the bucket, and this value is selected according to the contact between the bucket and the soil to ensure smoothness and stability during the excavation process and avoid unnecessary resistance. Consequently, the chosen parameters are: h_1 = 59 mm, h_2 = 96 mm, and h_3 = 15 mm. According to Figure 2, shovel length L is:

$$L = \frac{\mathrm{h}}{\sin\alpha} \tag{5}$$

Analysis of the digging shovel blade angle

The size of the inclination α of the shovel will affect the soil entry performance, soil breaking performance, excavation resistance and lifting height of the excavation blade (Fan, 2020; Li et al., 2021; Liu et al., 2019). A smaller blade angle decreases the friction between the digging shovel and the soil-potato mixture. However, if the blade angle is too small, the overall length of the digging shovel will increase. Therefore, the blade angle of the digging shovel should satisfy the following formula:

$$F_P \cos\alpha - F_f - G\sin\alpha \geq 0 \tag{6}$$

$$F_n - G\cos\alpha - F_p \sin\alpha = 0 \tag{7}$$

$$F_f = \tan\phi_1 F_n \tag{8}$$

Where:

ϕ_1 is the friction angle between soil and digging shovel, °.

By combining eqs (6), (7) and (8), we obtain:

$$\alpha \leq \arctan\frac{F_P - \tan\phi_1 G}{G + \tan\phi_1 F_P} \tag{9}$$

According to [eq. (9)], a smaller cutting angle α improves the soil entry performance and reduces the digging resistance, but the soil fragmentation performance is poor. Additionally, a smaller angle results in a longer digging shovel length to achieve a certain lifting height, which may cause soil accumulation. Conversely, a larger cutting angle α enhances soil fragmentation performance but worsens soil entry performance and increases digging resistance (Jia et al., 2023; Li et al., 2019). The curved shovel balances these factors: the front section AB has a smaller cutting angle α_1 to facilitate soil entry; the middle section BC has a larger cutting angle α_2 to enhance soil fragmentation and shorten the shovel length; and the rear section CD, which includes a stone guard, has a smaller cutting angle α_3 to loosen the compressed soil (Chen et al., 2024; Feng et al., 2022; Gierz et al., 2022). According to the industry standards for potato harvesters, the cutting angle α_1 is generally between 10° and 15°, α_2 is between 16° and 24°, and α_3 is between 12° and 15°. The lengths of each section are shown in Table 1.

TABLE 1. Shovel length data.

α_1（°）	L_1（mm）	α_2（°）	L_2（mm）	α_3（°）	L_3（mm）
10	340	16	348	12	72
11	309	17	328	13	67
12	284	18	311	14	62
13	262	19	295	15	58
14	244	20	281	\	\
15	228	21	268	\	\
\	\	22	256	\	\
\	\	23	246	\	\
\	\	24	236	\	\

Discrete element simulation model of an excavator shovel

The Discrete Element Method is a technique used to study the physical mechanisms of particle motion, and is particularly suitable for simulating the contact or collision processes of particle assemblies (Xin & Liang, 2022). The EDEM discrete element software is employed to simulate the interaction between soil particles and the digging shovel. Using spherical particles in the simulation closely replicates the physical characteristics of actual soil particles, enhancing the accuracy of the simulation and more realistically modeling the forces between moving particles.

Model data

During operation, both the soil and potatoes are scattered; hence the soil can be considered as particles of a certain size (Shen et al., 2023; Shkaruba et al., 2022). The simulation model consists of the digging shovel and soil. The angles of the shovel blades, α_1, α_2, and α_3, serve as the focus of the discrete element simulation to analyze the relationships between the differences in these angles. In this model, the thickness of the digging shovel is 6 mm. The lengths of the AB, BC, and CD sections of the shovel blade are specified in Table 1. Other parameters are consistent with previous settings, with soil dimensions being 800 mm in length, 320 mm in width, and 200 mm in height. The simulation model of the digging shovel in contact with the soil is illustrated in Figure 3.

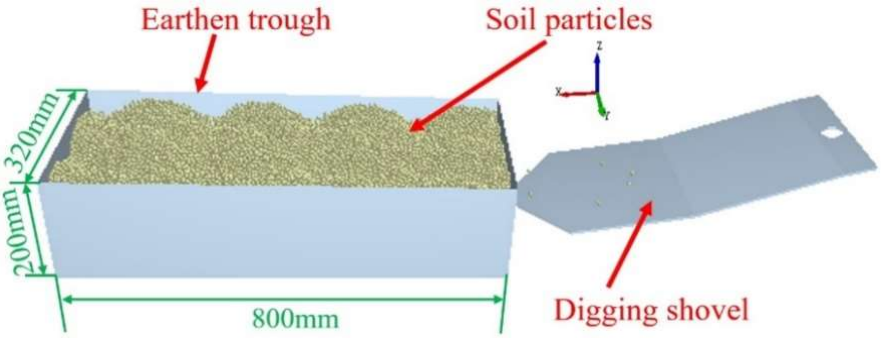

FIGURE 3. Digging shovel single shovel contact with soil model.

Calculation parameters

Mn65 steel is selected as the material for the digging shovel; the soil is clay from hilly areas (Lazzaro et al., 2023; Li et al., 2023; Zhou et al., 2022), and its specific parameters are shown in Table 2.

TABLE 2. Digging shovel and soil simulation calculation parameters.

Parameter	Numeric value
Poisson's ratio of soil particles	0.3
Shear modulus of soil particles (Pa)	1e+08
Density of soil particles (kg/m^3)	2680
Particle-to-particle recovery coefficient	0.3
The coefficient of rolling friction between particles and particles	0.3
The coefficient of static friction between particles	0.5
Recovery coefficient between the pellet and the digging blade	0.3
Coefficient of rolling friction between the pellet and the digging blade	0.2
Coefficient of static friction between particles and digging blade	0.3
Particle radius (mm)	3

The research focuses on the soil-digging shovel system, combined with the actual working condition of the potato harvester, the Hertz-Mindlin with Bonding contact model is chosen, with bonding model parameters detailed in Table 2 (Liu et al., 2023). The fixed simulation step is set to 20% of the Rayleigh step, with a total simulation time of 2.5 seconds and data saved every 0.01 s (Torotwa et al., 2023). The soil particles settle completely before the digging shovel begins to move, starting at 1.2 s and ending at 2.5 s. Various particle models are available in EDEM software; a simplified soil particle model is created for computational efficiency. In the simulation environment, soil particles fall for 1 s at a speed of 2 m/s, and the digging shovel moves horizontally for 1500 mm.

Particle size-independent analysis

As illustrated in Figure 4, to test the irrelevance of particle size, the simulation model uses digger blade angles $\alpha_1 = 10°$, $\alpha_2 = 20°$, and $\alpha_3 = 15°$, with particle radii ranging from 2 mm to 4 mm. When particle radii are between 3.5 mm and 4 mm, blade pressure, power, and forward resistance increase. With a radius of 3 mm, these parameters stabilize, showing minimal differences compared to a 2 mm radius: blade pressure differs by only 13.1 Pa, power by 0.01 W, and forward resistance by 0.29 N, significantly reducing computation time. Given efficiency and accuracy considerations, setting the simulation model's particle radius at 3 mm is deemed appropriate.

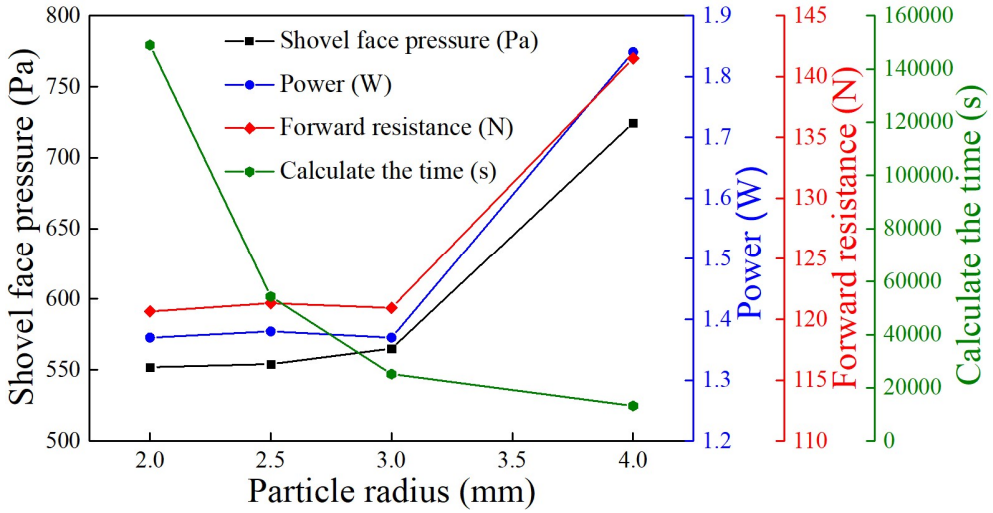

FIGURE 4. Mesh irrelevance analysis.

Analysis of the angular difference between the inclination angles α_1 and α_2 of the shovel face

Soil fragmentation capacity and forward resistance are critical factors determining the performance of digging shovels (Cui et al., 2019). Consequently, the angular difference Δ_1 between α_1 and α_2 can reflect the shovel's soil fragmentation ability to some extent. The effect of angular difference Δ_2 on Δ_1 is first determined. Subsequently, the angular ranges for α_1 and α_2 are set, and simulations for Δ_1 = 1°～9° are conducted. Analyses are carried out in terms of blade pressure, forward resistance, and power to determine the impact of Δ_1 on the performance of the digging shovel.

The effect of Δ_1 on the performance of the shovel face when Δ_2 varies

As Δ_1 changes, Δ_2 also varies. To explore the impact of Δ_1 on the overall digging performance of the shovel, after determining blade angles α_2 and α_3, the angle α_1 is varied to compare the blade pressure, power, and forward resistance for different Δ_1 values, as shown in Figure 5. When $\alpha_2 = 24°$, there is only one scenario, with $\Delta_1 = 9°$; hence it is not represented in the diagram; when $\alpha_1 = 15°$, $\alpha_2 = 24°$, $\alpha_3 = 13°$, the blade pressure is 838.13 Pa, the power is 1.40 W, and the forward resistance is 98.78 N.

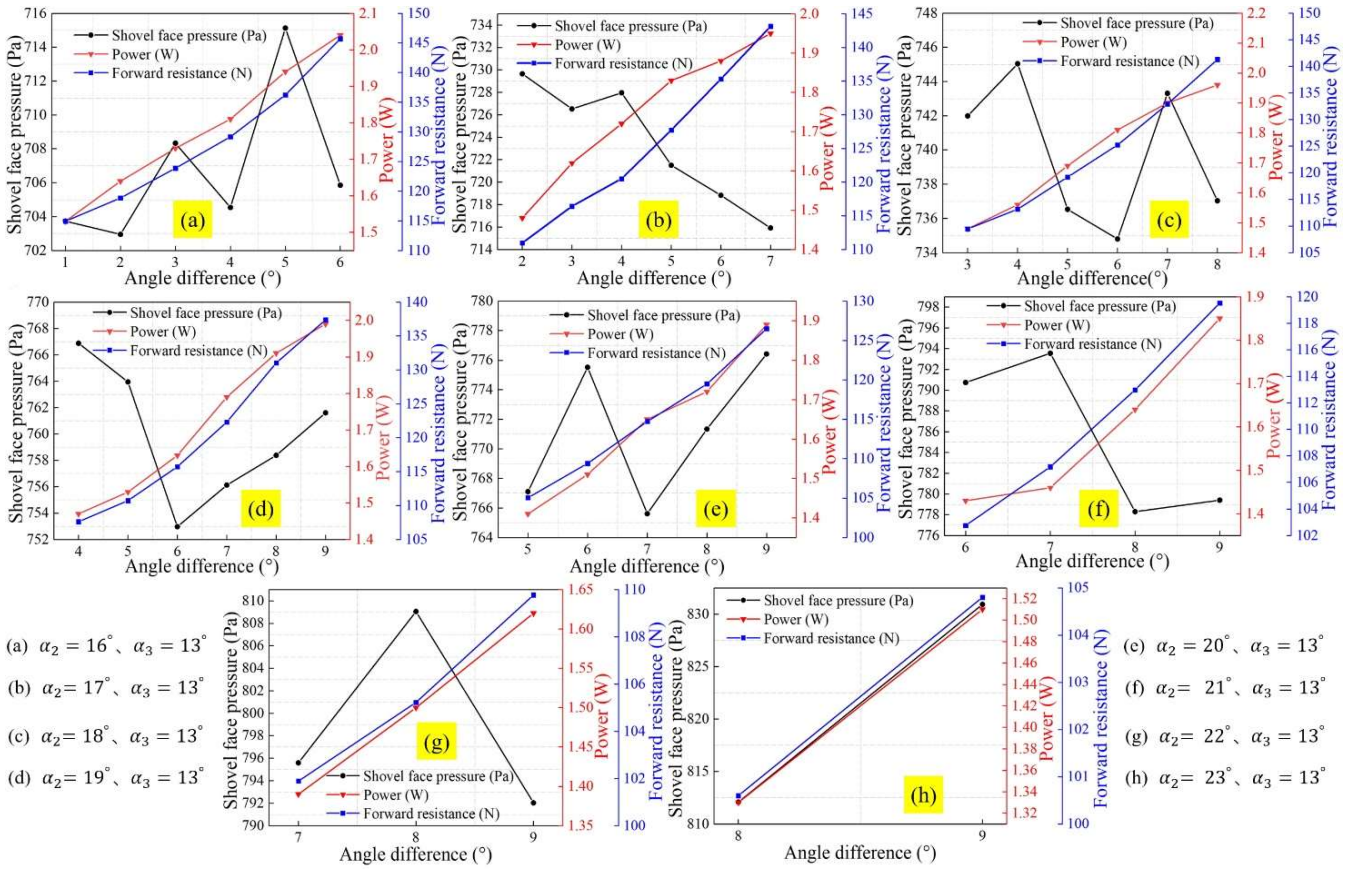

FIGURE 5. Angle difference when blade angles α_2 and α_3 are fixed.

In Figure 5, subfigures (a) to (h) correspond to the combinations α_2 of 16° ~ 23° and α_3 of 13°, respectively. Once α_2 and α_3 are determined, a larger angle difference Δ_1 results in higher power and forward resistance, but the blade pressure fluctuates significantly and exhibits large variations. As α_2 increases while α_3 remains constant, the maximum blade pressure for each group increases with α_2, but the maximum power and forward resistance decrease as α_2 increases.

To investigate the effects of different Δ_1 on overall blade pressure, power, and forward resistance under varying Δ_2, this study conducted a relative error analysis for each group's data when α_2 and α_3 are fixed, using the median values from Figure 5 as the baseline. As shown in Figure 6, the relative errors for blade pressure, power, and forward resistance change with variations in α_2. Specifically, the maximum relative error is: 2.27% for blade pressure, 22.09% for power, and 18.72% for resistance. This analysis demonstrates that Δ_1 has the least impact on blade pressure, a moderate impact on forward resistance, and the greatest impact on power.

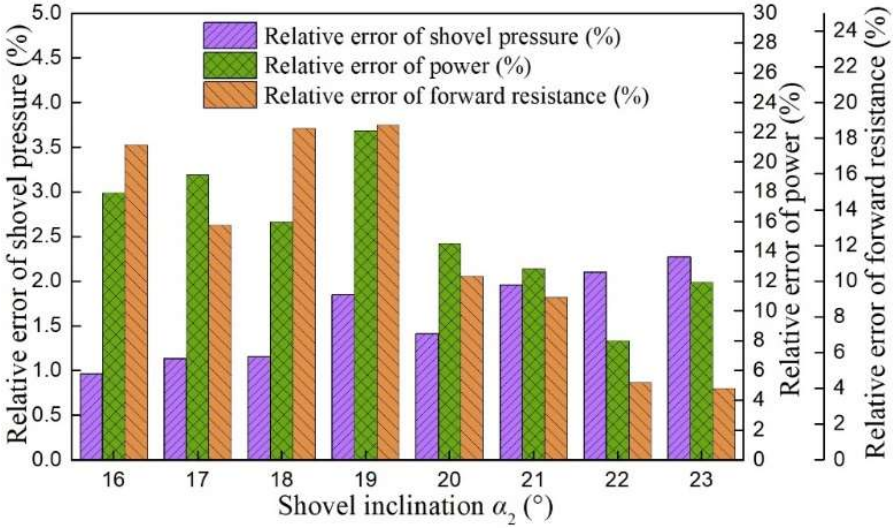

FIGURE 6. The maximum relative error of the performance of each shovel face at different Δ_2.

The influence of angle difference Δ_1 on the performance of the shovel surface

To explore the impact of varying angular difference Δ_1 on the performance of digging shovels, a comparative

analysis was conducted on the changes in blade pressure, power, and forward resistance with respect to Δ_1, under different combinations of blade angles where blade angle α_3 is fixed and angles α_1 and α_2 vary. Figure 7 displays the relationship between the performance of the digging shovel and the tilt angle α_2 as the angular difference Δ_1 ranges from 2° to 9°. Analysis of the figure aids in understanding how different Δ_1 angular differences influence the digging process, thereby optimizing blade design and enhancing the performance of digging shovels in operational conditions. The impact of angular difference Δ_1 on blade performance is depicted in Figure 7.

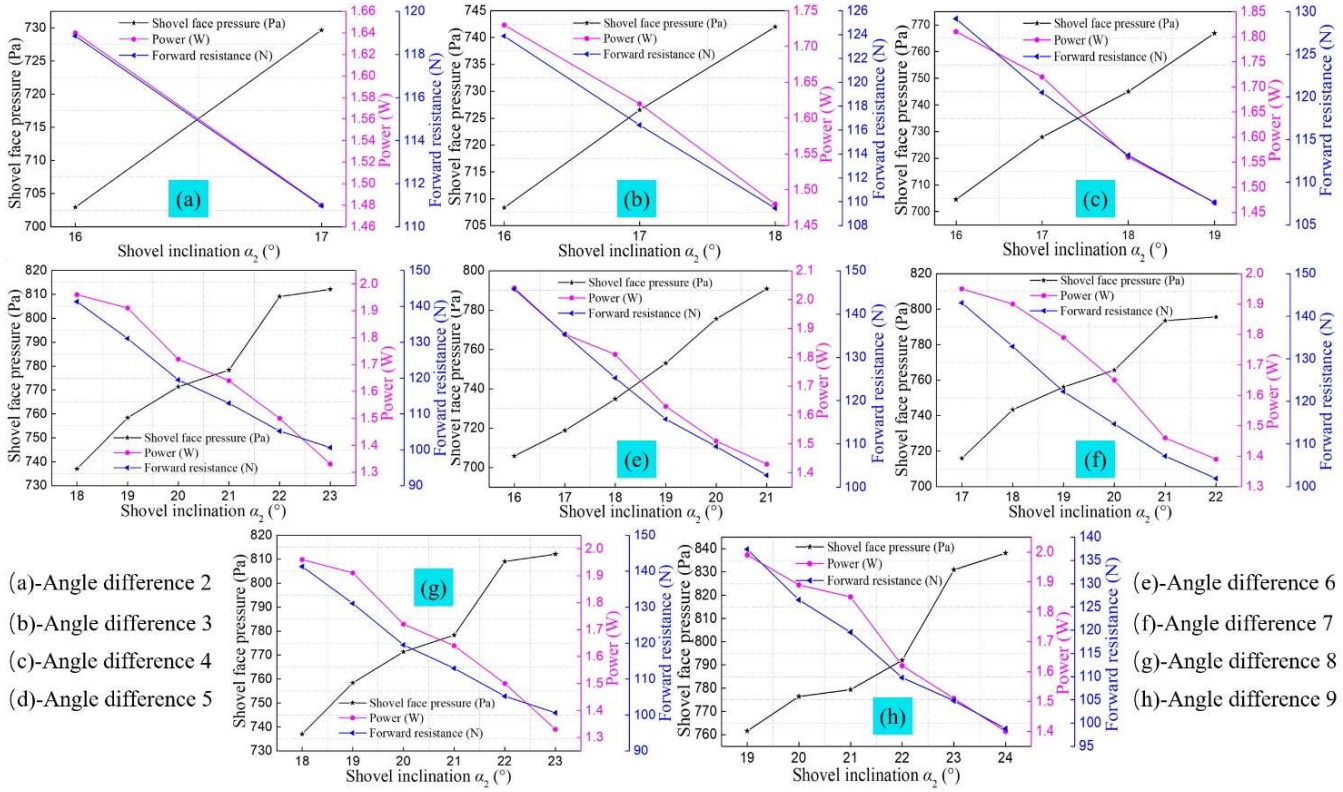

FIGURE 7. Comparison of simulation results with different angle differences Δ_1.

As illustrated in Figure 7, a certain relationship exists between blade pressure, power, and forward resistance. Under the same angular difference Δ_1, higher blade pressures correlate with lower power and forward resistance; furthermore, smaller blade angles α_1 and α_2 result in lower blade pressures, but higher power and forward resistance. When Δ_1 varies, with α_1 constant, larger Δ_1 results in greater blade pressure; however, with α_2 constant, Δ_1 has a minimal overall impact on blade pressure.

To explore the effects of different angular differences on overall excavation performance, the paper compares blade pressure, power, and forward resistance by averaging all simulation results for angular differences Δ_1 = 1° ~ 9°, as shown in Figure 8.

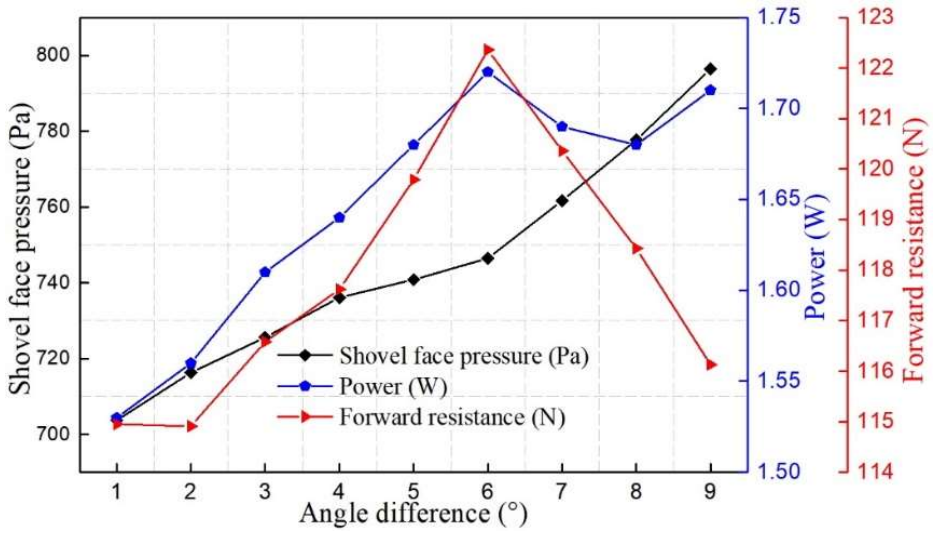

FIGURE 8. Average value of angular difference Δ_1.

As illustrated in Figure 8, the blade pressure increases with the increase in Δ_1. When Δ_1 = 1°~6°, the power and forward resistance also increase with the increase of the angle difference Δ_1. At Δ_1 = 6°, power and forward resistance peak at 1.72 W and 122.36 N, respectively. However, from Δ_1 = 7° ~ 9°, the forward resistance decreases with increasing Δ_1. When Δ_1 = 7° and Δ_1 = 8°, power decreases as Δ_1 increases, but at Δ_1 = 9°, power increases again to 1.71 W, only 0.01 W less than the maximum power observed.

The influence of the length of the excavation shovel on various factors

To explore the relationship between the blade length L of the digging shovel and the blade pressure, power, and forward resistance during the excavation process, a comparison of all simulation results at Δ_1 = 9° is presented in Figure 9.

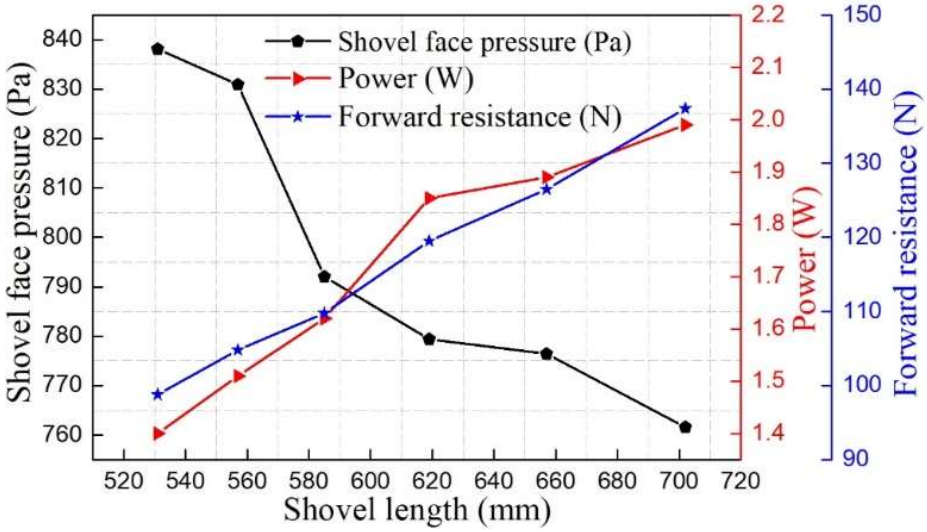

FIGURE 9. The impact of digging shovel blade length L on excavation performance.

Figure 9 illustrates that the blade length L is inversely proportional to the blade pressure, with longer L resulting in lower blade pressure. Conversely, L is directly proportional to both power and forward resistance, indicating that longer L increases both power and forward resistance. Therefore, L significantly impacts blade pressure, power, and forward resistance.

Analysis of the angular difference between the inclination angles α_2 and α_3 of the shovel face

Loosening capability is a key factor influencing the performance of excavation shovels (Cui et al., 2019). Thus, the angle difference Δ_2 can, to some extent, reflect the loosening capability of the shovel. The ranges for angles α_2 and α_3 were established, and simulations were conducted for blade angle combinations with Δ_2 ranging from 1° ~ 12°. The simulations analyzed blade pressure, forward resistance, and power to determine the impact of Δ_2 on the performance of the excavation shovel.

The effect of Δ_2 on the performance of the shovel surface when Δ_1 varies

To systematically study the impact of varying angle differences on blade pressure, power, and forward resistance, this research conducted a series of simulations analyzing different angle differences when blade angles α_2 and α_3 were the same, as shown in Figure 10. It displays the relationship between blade pressure, power, and forward resistance as the angle difference varies, with α_1 fixed at 13° and α_2 changing from 16° ~ 24°. Each subplot corresponds to different angle combinations, revealing the complex effects of angle differences on the excavation process.

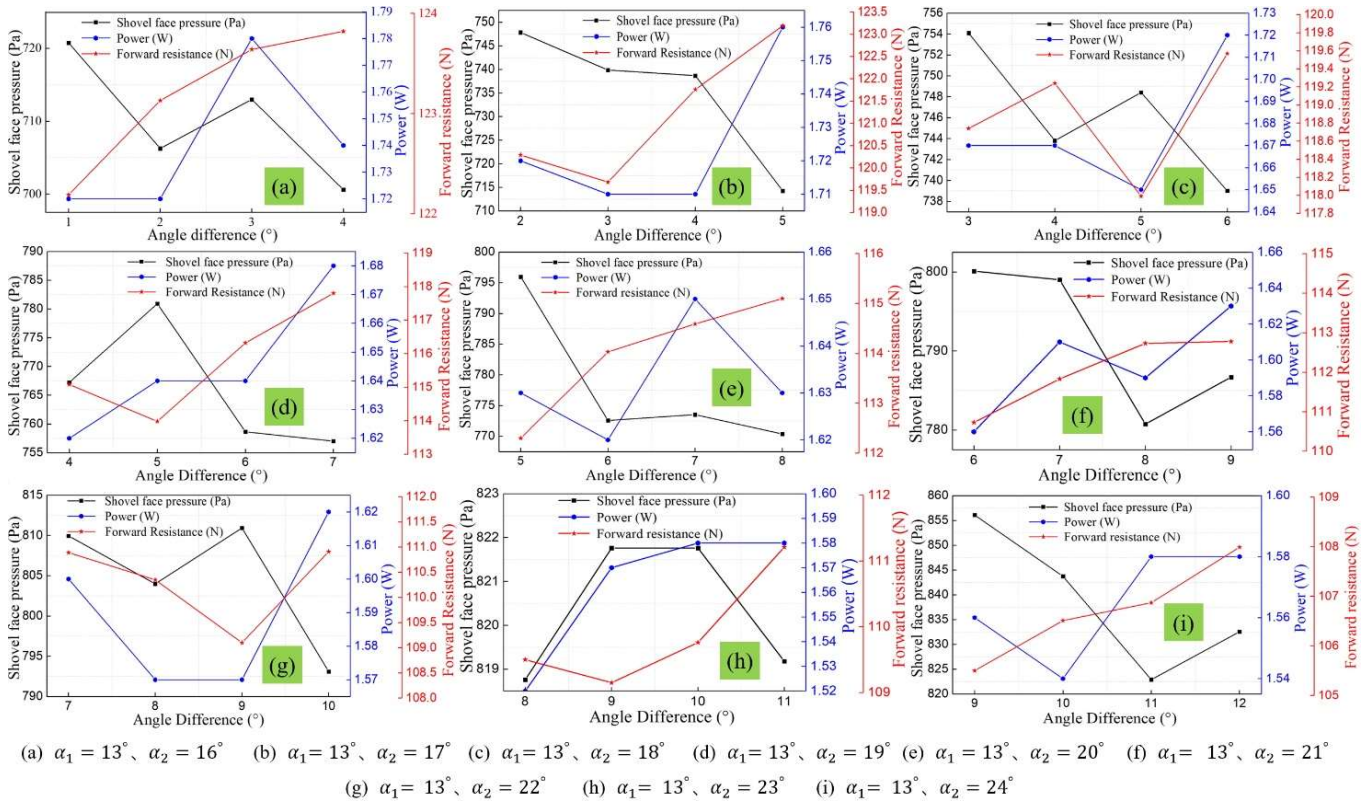

(a) $\alpha_1 = 13^\circ$、$\alpha_2 = 16^\circ$ (b) $\alpha_1 = 13^\circ$、$\alpha_2 = 17^\circ$ (c) $\alpha_1 = 13^\circ$、$\alpha_2 = 18^\circ$ (d) $\alpha_1 = 13^\circ$、$\alpha_2 = 19^\circ$ (e) $\alpha_1 = 13^\circ$、$\alpha_2 = 20^\circ$ (f) $\alpha_1 = 13^\circ$、$\alpha_2 = 21^\circ$
(g) $\alpha_1 = 13^\circ$、$\alpha_2 = 22^\circ$ (h) $\alpha_1 = 13^\circ$、$\alpha_2 = 23^\circ$ (i) $\alpha_1 = 13^\circ$、$\alpha_2 = 24^\circ$

FIGURE 10. Angle difference when digging shovel blade angles α_1 and α_2 are fixed.

Figure 10 illustrates the relationship between blade pressure, power, and forward resistance under different angle differences Δ_1 as Δ_2 changes. Subfigures (a) to (i) sequentially correspond to combinations when $\alpha_1 = 13°$, with α_2 ranging from 16° to 24°. The overall trend indicates that as the angle difference Δ_2 increases, blade pressure and power exhibit nonlinear fluctuations, while forward resistance significantly increases at certain angle differences, particularly under larger angle difference conditions. Subfigure (a) shows maximum forward resistance at $\Delta_2 = 4°$; subfigure (b) records the highest forward resistance at $\Delta_2 = 5°$; from subfigures (c) to (i), the power and forward resistance differ at the points where Δ_2 reaches their respective maximums, reflecting the complex impact of Δ_1 on the excavation process.

To ascertain the impact of angle difference Δ_2 on overall blade pressure, power, and forward resistance at different Δ_1, this study used the median values from Figure 10 as baseline values and calculated the relative errors for each set under different Δ_1. Figure 11 depicts the percentage of relative errors in blade pressure, power, and forward resistance under different Δ_1. The results indicate significant increases in the relative errors for blade pressure and power at certain angles, such as blade inclinations α_2 of 18°, 19°, and 21°, while the errors for forward resistance are relatively lower and more stable. Overall, forward resistance exhibits better stability, whereas blade pressure and power show larger fluctuations; yet all remain under 4%, indicating that different values of Δ_1 have minor effects on blade performance analysis.

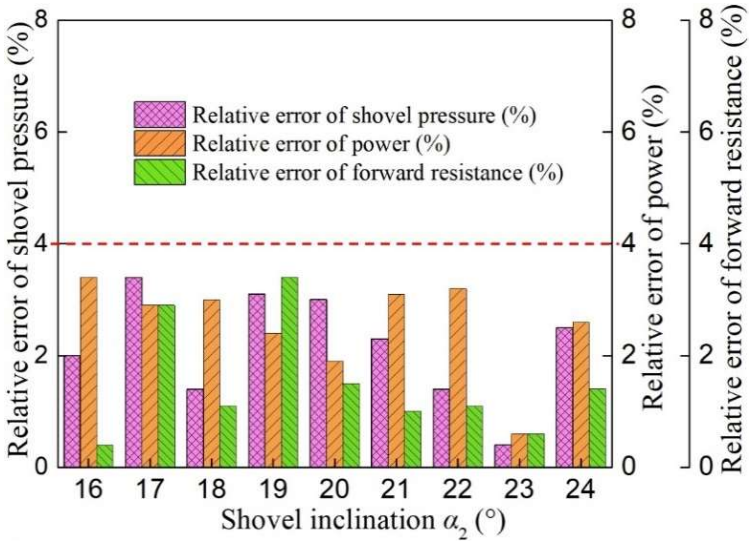

FIGURE 11. The maximum relative error of the performance of each shovel face at different α_2.

The influence of different angle difference Δ_2 on the performance of the shovel surface

Due to the minimal impact of Δ_1 on Δ_2 analysis, this study focuses on comparing simulations with the same Δ_2, as shown in Figure 12. The figure displays the relationship between blade pressure, power, and forward resistance as α_2 changes, within a range of Δ_2 from 2° to 11°. When the angle difference Δ_2 is 1°, the only scenario is α_2 = 16°, α_3 = 15°; when Δ_2 is 12°, the only scenario is α_2 = 24°, α_3 = 12°, and hence these are not depicted in Figure 12. With α_1 = 13°, α_2 = 16°, α_3 = 15°, the blade pressure is 720.73 Pa, power is 1.72 W, and forward resistance is 122.19 N; with α_1 = 13°, α_2 = 24°, α_3 = 12°, the blade pressure is 832.54 Pa, power is 1.58 W, and forward resistance is 107.99 N. Generally, as α_2 increases, blade pressure and forward resistance show varying trends of decline, while power exhibits relatively larger fluctuations. Subfigures (a) to (c) illustrate that at smaller Δ_2 (2° ~ 4°), blade pressure and forward resistance gradually decrease, whereas power remains relatively stable; subfigures (d) and (e) indicate that as Δ_2 increases to 5° and 6°, significant fluctuations appear in power and forward resistance, with a notable reduction in blade pressure; subfigures (f) to (h) show that as Δ_2 further increases (7° ~ 9°), power significantly rises, and forward resistance sharply drops at larger α_2; subfigures (i) and (j) reveal more complex relationships among the three variables when Δ_2 reaches 10° and 11°, with continuing declines in blade pressure and forward resistance, while power fluctuates distinctly at different α_2. These results demonstrate that Δ_2 significantly affects the performance of the digging shovel, with blade pressure increasing and forward resistance decreasing as α_2 increases.

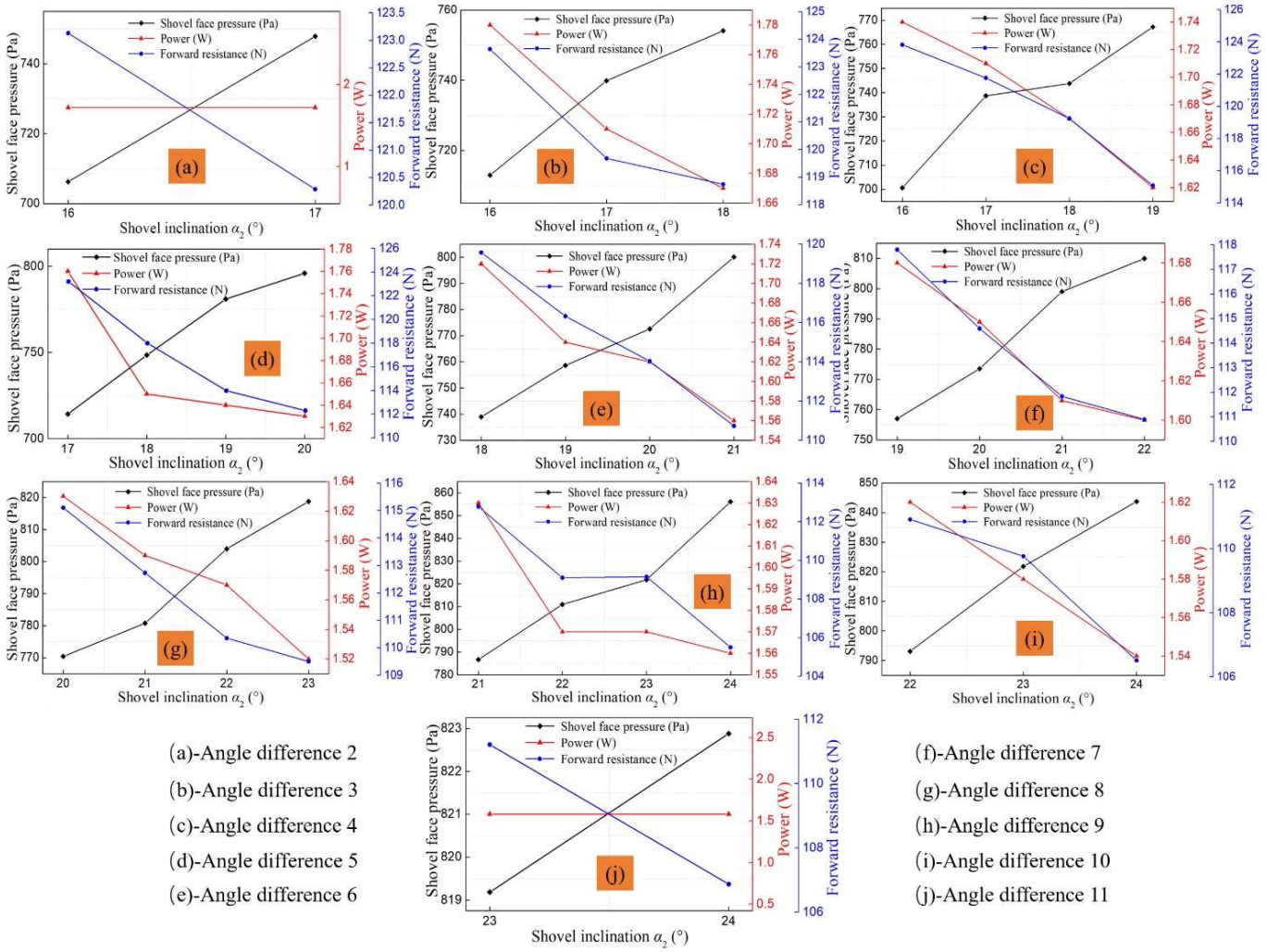

FIGURE 12. Comparison of simulation results t various fixed values of Δ_2.

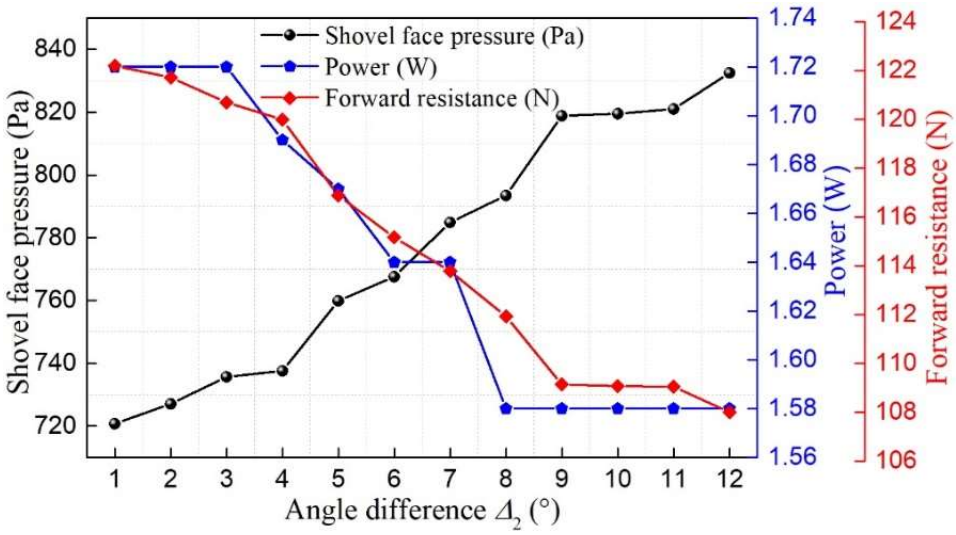

FIGURE 13. The average value of shovel pressure, power, and forward resistance.

To investigate the influence of different Δ_2 on overall excavation performance, this study averaged all simulation results for Δ_2 ranging from 1° to 12° and compared blade pressure, power, and forward resistance, as illustrated in Figure 13. It displays the relationship between blade pressure, power, and forward resistance as the angle difference Δ_2 varies from 1° to 12°. It is observed that blade pressure progressively decreases with an increase in Δ_2 from 1° to 12°, showing a clear negative correlation, particularly rapid declines between Δ_2 of 5° to 8°. Power remains relatively stable from 1° to 6° but significantly increases once Δ_2 exceeds 6°, indicating increased power demands due to excavation. Forward resistance sharply falls within the 1° to 8° range and stabilizes after Δ_2 exceeds 8°. This trend suggests that as Δ_2 increases, significant changes occur in resistance and power generated by excavation, with Δ_2's impact on blade pressure and forward resistance being especially notable. Within a certain Δ_2 range, the shovel operates with high efficiency and lower power consumption.

CONCLUSIONS

Based on the above analysis, the following conclusions can be drawn:

(1) Blade pressure increases with the increase in angle difference Δ_1. From $\Delta_1 = 1° \sim 6°$, power and forward resistance also increase with the angle difference, but from $\Delta_1 = 6° \sim 9°$, power fluctuates and forward resistance gradually decreases.

(2) The impact of angle difference Δ_1 is minimal on blade pressure, more significant on forward resistance, and greatest on power.

(3) Blade length is directly proportional to power and forward resistance but inversely proportional to blade pressure.

(4) With the increase in angle difference Δ_2, significant changes occur in the resistance and power required for excavation. The impact of Δ_2 is particularly notable on blade pressure and forward resistance. Within a certain range of angle difference Δ_2, the blade operates with higher efficiency and lower power consumption.

The blade inclination optimization method proposed in this paper provides an effective theoretical basis for improving excavation efficiency and reducing power consumption. By analyzing the impact of different angular differences and blade lengths on blade performance, research has shown that blade design can achieve higher productivity by optimizing these parameters. Under complex soil conditions and uneven terrain, this method can effectively improve the working performance of shovel blades and reduce energy consumption, and it has a degree of universality.

In this paper, through the systematic analysis of parameters such as angular difference and blade length, it provides a new theoretical basis for the design of shovel blades and the optimization of excavation efficiency. The results show that the angular difference and blade length have a significant impact on the power, forward resistance and blade pressure; in particular, the angular differences Δ_1 and Δ_2 have greater impacts on the blade performance. Specifically, changes in angular difference significantly affect blade efficiency and energy consumption, while changes in blade length are proportional to power and forward resistance. The model in this paper provides actionable optimization directions for blade design, helping to improve digging efficiency and reduce power consumption.

Future research can further expand the application of the model on this basis, and combine multi-factor analysis and actual working conditions to improve the practical application value of the model.

ACKNOWLEDGEMENTS

This work was supported by the Design of a trailed potato harvester in hilly terrain (No. XDNY2023-007).

REFERENCES

Bao, G. H., Wang, G. P., Wang, B., Hu, L. L., Xu, X. W., Shen, H. Y., & Ji, L. L. (2021). Study on the drop impact characteristics and impact damage mechanism of sweet potato tubers during harvest. *Plos One*, 16(8), e0255856

Cao, C. M., Liu, Z. B., Ding, W. Y., Wu, M., Zhang, X. C., & Qin, K. (2023). Design and experiment of ning-guo radix peucedani bionic digging shovel. *Transactions of the Chinese Society for Agricultural Machinery*, 54(11), 102–113.

Chen, M. D., Liu, X. T., Hu, P. X., Zhai, X. T., Han, Z. L., Shi, Y. L., Zhu, W. J., Wang, D. W., He, X. N., & Shang, S. Q. (2024). Study on rotor vibration potato-soil separation device for potato harvester using dem-mbd coupling simulation. *Computers and Electronics in Agriculture*, 218. https://doi.org/10.1016/j.compag.2024.108638.

Clarke, J. (2022). Enhancing the performance of potato harvesters with hybrid shovel blades. *Agricultural Mechanics Worldwide*, 88(2), 154–162.

Cui, G., Ma, Y. H., Yang, D. Q., Jia, J. X., & Li, Y. (2019). Research situation of bionic resistance reducing technology about potato digging shovel. *Agricultural Engineering*, 9(09), 19–22.

Dun, G. Q., Sheng, Q. B., Ji, X. X., Jiang, X. B., Zhao, Y., & Zhou, C. (2023). Optimization and experiment of staggered gear manure spreader. *Journal of Agricultural Engineering*, 39(20), 20–27.

Fan, Y. (2020). Research on the digging mechanism of potato harvesters and bionic shovel design based on the discrete element method. *Journal of Shenyang Agricultural University*.

Feng, X., Chen, L., Li, M. T., & Xiang, J. (2022). Design and test of potato soil separation device based on potato harvester. Proceedings of the 2022 3rd International Conference on Artificial Intelligence in Electronics Engineering,1 - 8. https://doi.org/10.1145/3512826.3512827

Ge, Y. Y., Jiao, H. C., Liu, D. X., Liang, Q. Y., & Yang, C. H. (2023). Simulation and experiment of straw-soil particle turnover movement based on EDEM. *Journal of Chinese Agricultural Mechanization*, 44(7), 229–235.

Gierz, M., Przybyl, K., Koszela, K., Duda A., & Szychta, M. (2022). Analysis of the strength of an innovative design of an organic farming potato harvester. *Journal of Physics: Conference Series*, 2212(1), https://doi.org/10.1088/1742-6596/2212/1/012028

Jia, B. X., Sun, W., Zhao, Z. W., Wang, H. C., Zhang, H. L., Liu, X. L., & Li, H. (2023). Design and field test of a remotely controlled self-propelled potato harvester with manual sorting platform. *American Journal of Potato Research*, 100(3), 193–209.

Lazzaro, U., Mazzitelli, C., Sica, B., Di Fiore, P., Romano, N., & Nasta, P. (2023). On evaluating the hypothesis of shape similarity between soil particle-size distribution and water retention function. *Journal of Agricultural Engineering*, 54(4).

Li, J. W., Gu, T. L., Li, X. Y., Wang, Z. J., Hu, B., & Ma, Y. (2023). Analysis and experiment of the bionic drag reduction characteristics of potato digging shovels on clayey black soil conditions. *Transactions of the Chinese Society of Agricultural Engineering*, 39(20), 1–9.

Li, T., Li, N., Liu, C. G., Zhu, Z. B., Zhou, J., & Zhang, H. (2021). Development of automatic depth control system employed in potato harvester. *Transactions of the Chinese Society for Agricultural Machinery*, 52(12), 16–23.

Li, X. P., Liao, M., Hu, B., Pan, Q. L., & Tao, J. J. (2019). Research on bionic digging shovel blades for potatoes and their drag reduction characteristics. *Journal of Agricultural Mechanization Research*, 41(6), 8.

Liu, L., Wang, X. L., Zhong, X. K., Zhang, X. C., Geng, Y. L., Zhou, H., & Chen, T. (2023). Design and experiment of furrow side pick-up soil blade for wheat strip-till planter using the discrete element method. *Journal of Agricultural Engineering*, 55(1), https://doi.org/10.4081/jae.2023.1546.

Liu, P. F., Liu, Z. G., Pei, C. H., Yang, L., Zhang, S. Y., & Duan, M. Z. (2019). Design optimization and reliability analysis of hydraulic cleaning system for potato harvester. International Conference on Quality, Reliability, Risk, Maintenance, and Safety Engineering, https://doi.org/10.1109/QR2MSE46217.2019.9021143.

Müller, H., & Schmidt, B. (2019). Field performance of adjustable blade angle shovels in potato harvesting equipment. *European Journal of Agronomy*, 110, 126–134.

Park, D., Lee C., Park, H., Baek, S., & Rhee, J. (2019). Discrete element method analysis of the impact forces on a garlic bulb by the roller of a garlic harvester. *Journal of Biosystems Engineering*, 44(4), 208–217.

Shen, H. Y., Wang, B., Wang, G. P., Wang, Y. M., Bao, G. C., Hu, L. L., & Hu, Z. C. (2023). Research and optimization of the hand-over lifting mechanism of a sweet potato combine harvester based on EDEM. *International Journal of Agricultural and Biological Engineering*, 16(5), 71–79.

Shkaruba, N., Leonov, O., & Bogolubova, D. (2022). Quality indicators influencing the choice of potato harvester. *IOP Conference Series: Earth and Environmental Science*, 981.

Tan, X. Z., Zhang, B., Shen, C. J., Fu, W., & Meng, H. W. (2023). Parameter optimization and experimentation of vibratory subsoiling tillage machines based on EDEM. *Journal of Agricultural Mechanization Research*, 45(9), 7.

Thomas, R., & Fischer, S. (2020). Application of UHMWPE coatings on agricultural digging tools to minimize wear and soil adhesion. *Journal of Agricultural Engineering Research*, 96(3), 45–52.

Torotwa, I., Ding, Q., Awuah, E., & He, R. (2023). Biomimetic tool design improves tillage efficiency, seedbed quality, and straw incorporation during rototilling in conservation farming. *Journal of Agricultural Engineering*, 54(1), https://doi.org/10.4081/jae.2023.1327.

Wang, F., Cao, Q. Z., Li, Y. B., Pang, Y. L., Xie, K. T., & Zhang, Z. G. (2023a). Design and trafficability experiment of self-propelled potato harvester in hilly and mountainous areas. *Transactions of the Chinese Society for Agricultural Machinery*, 54(s2), 10–19.

Wang, H. Y., Zhang, Z. G., Ibrahim, I., Xie, K., Wael, E., & Cao, Q. (2021). Design and experiment of small-sized potato harvester suitable for hilly and mountainous areas. *Acta Agricultural Zhejiangensis*, 33(04), 724–738.

Wang, X., Yang, D. Q., Liu, M. M., Li, Y., Chen, X. Y., & Cheng, Z. W. (2023b). Optimization and experimentation of pickup device parameters for self-propelled potato harvester. *Transactions of the Chinese Society for Agricultural Machinery*, 54(S02), 20–29.

Wei, J. (2024). Virtual design and simulation of 4U-1A potato harvester. IEEE. https://doi.org/10.1109/CAIDCD.2009.537508.

Wei, Z. C., Wang, X. H., Li, X. Q., Wang, F. M., Li, Z. H., & Jin, C. Q. (2023). Design and experiment of crawler self-propelled sorting type potato harvester. *Transactions of the Chinese Society for Agricultural Machinery*, 54(02), 95–106.

Wei, Z. C., Li, H. W., Su, G. L., Sun, C. Z., Liu, W. Z., & Li, X. Q. (2019). Design and experiment of potato harvester using double cushions for low laying separation technology. *Transactions of the Chinese Society for Agricultural Machinery*, 50(09):140-152.

Wilson, P., Davis, L., & Roberts, K. (2021). Optimizing potato harvester shovel designs using computational fluid dynamics. *International Journal of Mechanical Engineering*, 17(4), 237–245.

Wu, F. (2022). DEM-MBD coupling simulation and analysis of the working process of soil and tuber separation of a potato combine harvester. *Agronomy*, https://doi.org/12.10.3390/agronomy12081734.

Xin, L. L., & Liang, J. H. (2022). Design of conveyor separation device for potato harvester and analysis of its vibration characteristics. *Journal of computational methods in sciences and engineering*, 22(4),1385-1392.

Xu, L. H., Wei, C. C., Liang, Z. W., Chai, X. Y., Li, Y. M., & Liu, Q. (2019). Development of rapeseed cleaning loss monitoring system and experiments in a combine harvester. *Biosystems Engineering*, 178(000), 13.

Ye, D. P., Zhao, J. N., Qing, J. X., Shen, B. H., Weng, H. Y., & Zheng, S. H. (2023). Design and experiment of key components of an electric spiral-type small fertilizer machine based on EDEM. *Journal of Shenyang Agricultural University*, 54(1), 81–89.

Yi, J., Zhou, B., & Wei, X. R. (2023). Analysis of discharge uniformity in vibrating screens using EDEM Discrete Element Simulation. *Journal of Mechanical Design and Manufacture*, 12, 55.

Zbanov, N., Kostenko, M., Kostenko, N., & Rembalovich, G. (2020). Justification of the rigidity of composite bars of a potato harvester elevator. *Polythematic Online Scientific Journal of Kuban State Agrarian University*, https://doi.org/10.21515/1990-4665-158-016.

Zhang, C., Fan, X. H., Li, M. S., Li, G., Zhao, C. K., & Sun, W. L. (2022). Simulation analysis and experiment of soil disturbance by chisel plough using EDEM. *Transactions of the Chinese Society for Agricultural Machinery*, 53(S02), 8.

Zhou, W., Ni X., Song, K., Wen, N., Wang, J. W., Fu, Q., Na, M. J., Tang, H., & Wang, Q. (2023). Bionic optimization design and discrete element experimental design of carrot combine harvester ripping shovel. *Processes*, 11(5). https://doi.org/10.3390/pr11051526

Zhou, Y., Qin, D. L., Li, Q. Q., Nie, J. S., Luo, H. Z., & Zhang, L. H. (2022). Optimization design and experiment of Job's tears vibrating screen cleaning device based on EDEM. *Journal of Northeast Agricultural University*, 53(11), 9.